Design and Modeling of a Numerical Simulator of a Mini-hydropower for Performance Characterization of the Turbine Type of Francis, Cross-flow and Pelton

Francis Kifumbi[1], Guyh Dituba Ngoma[1], Python Kabeya[2] and Clement N'zau Umba-di-Mbudi[3]
[1]*University of Quebec in Abitibi-Témiscamingue, School of Engineering, Rouyn-Noranda, Canada*
[2]*University of Kinshasa, Faculty of Polytechnic, Kinshasa, Democratic Republic of the Congo*
[3]*University of Kinshasa, Faculty of Science, Kinshasa, Democratic Republic of the Congo*

Keywords: Hydraulic Turbine, Blades, Buckets, Draft Tube, Cavitation, ANSYS-CFX, Computational Fluid Dynamic (CFD).

Abstract: This research work deals with the design of a numerical simulator which consists of an upstream reservoir, a penstock, a Francis turbine, a cross-flow turbine, a Pelton turbine, and a draft tube. This simulator can allow to better study the performance of a mini-hydroelectric plant while investigating the parameters involved with the cavitation phenomenon for the Francis turbine. From existing reference data of the gross head, the flow rate and the rotating speed for the Francis turbine, the cross-flow turbine and the Pelton turbine, the geometrical parameters of the turbine runners were calculated using inter alia the specific speeds, the turbines diagrams and the empirical equations. Moreover, the equations of continuity and Navier-Stokes are applied to obtain by means of the ANSYS-code the fields of the liquid flow velocity and the pressure. The numerical results achieved for the turbine output power and the efficiency were compared with the experimental results from the existing test benches of turbines in the turbomachinery facility of the Engineering School at the University of Quebec in Abitibi-Témiscamingue (UQAT). Also, the effect of the cavitation on the efficiency of the Francis turbine account for the draft tube height is analyzed. The impact of the draft tube height of the Francis turbine and the jet width of the cross-flow turbine on the output power and the efficiency is examined.

1 INTRODUCTION

The decentralized production of electricity from renewable sources is evolving very significantly and is constantly increasing day by day, reducing the dependency on fossil fuels and the production of greenhouse gases. The realization of the big hydroelectric power stations having become difficult due inter alia to the scarcity of sites and environmental restrictions on a world scale. That brings out the necessity to develop mini-hydropower plants with power lower to 10 MW.

Several research works that made objects of publication have been achieved on the morphology of the turbine components of the mini hydroelectric power stations. A review of low head micro-hydropower turbines was done focusing on the categories, the performance, the operation and the cost (Elbatran et al., 2015). The geometrical and structural study of the mechanical constraints that the blades of a cross-flow turbine undergo in full charge was done (Zanette, 2010). It was found that the mechanical stress sustained by the blades depends on the basic geometrical specifications of the cross-flow turbine, the rotating speed, the exact geometry of the blades and the velocity of the upstream water current. In addition, the author (Bartle, 2002) presented the current role that hydropower is playing in the world, along with some its inherent benefits, and then looks at the remaining potential, and some specific development plans in various regions of the world. Attention was drawn to the advantages of developing hydropower as part of a multipurpose water resources scheme, often enabling it to subsidize other valuable functions of a reservoir or river system. In the article (Olgun, 2000), it was investigated the effects of shape of guidance tubes to the interior of the cross-flow turbine and they achieved another parametric study

Kifumbi, F., Ngoma, G., Kabeya, P. and Umba-di-Mbudi, C.
Design and Modeling of a Numerical Simulator of a Mini-hydropower for Performance Characterization of the Turbine Type of Francis, Cross-flow and Pelton.
DOI: 10.5220/0011265000003274
In *Proceedings of the 12th International Conference on Simulation and Modeling Methodologies, Technologies and Applications (SIMULTECH 2022)*, pages 226-233
ISBN: 978-989-758-578-4; ISSN: 2184-2841

on the influence of the nozzle width according to the width of the runner and the blade number (Olgun, 1998).

Moreover, the study of Pelton turbines was deeply developed (Zhang, 2016) inter alia in terms of the injector characteristics, the interaction between the jet and Pelton runner, the hydraulic design of Pelton turbines, and the bucket mechanical strength and similarity laws. In the article (Panthee et al, 2014), the CFD analysis of scaled Pelton turbine Hydropower was performed using ANSYS CFX software to determine the torque generated by the turbine and the pressure distributions in the bucket. It was found that the torque results obtained from the single bucket can be replicated over time to predict the total torque transferred by the Pelton turbine. The study of (Židonis et al., 2015) was based on the influence of the bucket number of a Pelton turbine for the mini-hydropower plant, the interaction of the water jet on the runner in rotation and finally to make a comparison between the numerical results of the Ansys-CFX and ANSYS-Fluent codes. Furthermore, in the article (Kaewnai et al., 2011), the study to improve the runner design of Francis turbine and analyze its performance using Computational Fluid Dynamics was accomplished. In the article (Alligne et al., 2014), it was investigated the cavitation surge modelling in Francis turbine draft tube. Thus, the parametric analysis of the draft tube model was carried out to examine the influence of turbine variables on the cavitation surge onset identified by the hydraulic system stability. In addition, The Francis turbine was studied considering the speed variation (Trivedi et al., 2020). A particular focus was given to the inception of cavitation. The work showed specific instances of cavitation, where the large part of the turbine was cavitating intensely, including stay vane and guide vane passages. It was found that the cavitation becomes intense while crossing the threshold value of rotating speed.

Despite the described previous works, a numerical model of hydroelectric mini-power stations provided with the Francis turbine, cross-flow turbine and Pelton turbine being able to serve as a numerical test bench is not investigated. Therefore, in this research work, it is to develop a numerical simulator to study turbine characteristics under different operating conditions for the turbine type of Francis, cross-flow and Pelton. The first step of the research is focused on the turbine runners as presented in this paper.

2 MODEL DESCRIPTION

The model of the mini-hydropower considered in this work is illustrated in Figure 1. It is composed, inter alia, of an upstream reservoir, a downstream reservoir, a penstock and one of the three types of the turbine: Francis, Cross-flow and Pelton.

The solid models of the turbine runners are shown in Figure 2.

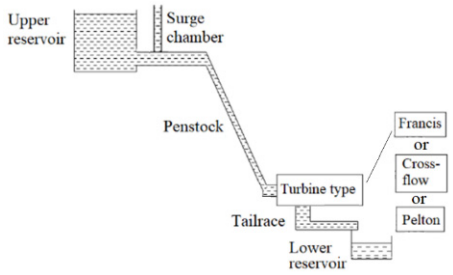

Figure 1: Model of the mini-hydropower.

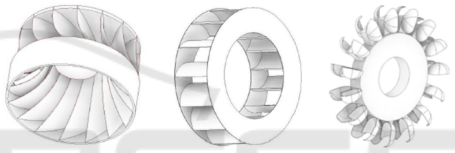

a) Francis b) Cross-flow c) Pelton

Figure 2: Solid models of the turbine runners.

3 MATHEMATICAL FORMULATION

To determinate the field of the liquid flow velocity and the field of the pressure in the hydraulic turbines, the following assumptions are considered for the liquid flow: (a) a steady state, three-dimensional and turbulence flow using the k-ε model is assumed; (b) the liquid is an incompressible liquid; (c) it is a Newtonian liquid; and (d) the liquid's thermophysical properties are constant with the temperature.

3.1 Equation of the Continuity

The equation of the continuity (Malonda et al., 2021) is given by:

$$\frac{\partial u}{\partial x}+\frac{\partial v}{\partial y}+\frac{\partial w}{\partial z}=0 \quad (1)$$

where u(x,y,z), v(x,y,z) and w(x,y,z) are the components of the liquid flow velocity U(u,v,w).

3.2 Equations of Navier-Stokes

The equations of the Navier-Stokes (Malonda et al., 2021) are written as follows:

$$\begin{aligned}
\rho\left(u\frac{\partial u}{\partial x}+v\frac{\partial u}{\partial y}+w\frac{\partial u}{\partial z}\right)&=\mu_{eff}\left(\frac{\partial^2 u}{\partial x^2}+\frac{\partial^2 u}{\partial y^2}+\frac{\partial^2 u}{\partial z^2}\right)\\
&\quad-\frac{\partial p}{\partial x}+\rho(\omega_z^2 r_x+2\omega_z v)+\rho g_x\\
\rho\left(u\frac{\partial v}{\partial x}+v\frac{\partial v}{\partial y}+w\frac{\partial v}{\partial z}\right)&=\mu_{eff}\left(\frac{\partial^2 v}{\partial x^2}+\frac{\partial^2 v}{\partial y^2}+\frac{\partial^2 v}{\partial z^2}\right)\\
&\quad-\frac{\partial p}{\partial y}+\rho(\omega_z^2 r_y-2\omega_z u)+\rho g_y\\
\rho\left(u\frac{\partial w}{\partial x}+v\frac{\partial w}{\partial y}+w\frac{\partial w}{\partial z}\right)&=\mu_{eff}\left(\frac{\partial^2 w}{\partial x^2}+\frac{\partial^2 w}{\partial y^2}+\frac{\partial^2 w}{\partial z^2}\right)\\
&\quad-\frac{\partial p}{\partial z}+\rho g_z
\end{aligned} \tag{2}$$

where g (g_x,g_y,g_z) is the gravity acceleration, p is the pressure; ρ is the density; μ_{eff} is the effective viscosity accounting for turbulence, it is defined as $\mu_{eff}=\mu+\mu_t$. μ is the dynamic viscosity and μ_t is the turbulence viscosity. It is linked to turbulence kinetic energy k and dissipation ε.

Equations 1 and 2 are solved by means of the ANSYS CFX-code (ANSYS inc., 2022) to obtain the fields of liquid flow velocity and pressure in hydraulic turbines.

4 DESIGN PARAMETERS OF THE HYDRAULIC TURBINES

4.1 Turbine Runners

To design the turbine runners, several parameters must be taken in account, inter alia, the water head, the flow rate, the rotating speed, the specific speed, the speed triangles and the cavitation factor. The type of the turbine runner depends on the specific speed (Peng, 2008). Moreover, the synchronous rotating speed of the turbine when the generator is directly coupled with the turbine can be determined by:

$$N=120fn_p^{-1} \tag{3}$$

where f is the electrical frequency and n_p is the even number of the generator poles.

The specific speed is the parameters that characterize the hydraulic turbines. It is expressed with the help of the Equations 4 and 5 according to:
a) the output power

$$N_s=N\frac{P_s^{\frac{1}{2}}}{H^{\frac{5}{4}}} \tag{4}$$

b) the flow rate

$$N_q=N\frac{Q^{\frac{1}{2}}}{H^{\frac{3}{4}}} \tag{5}$$

where P_s is the output power, N is the rotating speed, H is the net water head and Q is the flow rate.

Using Equation 4, the turbine type is found in Table 1.

Table 1: Turbine type (Peng, 2008).

Turbine type	Specific speed
	Ns [rpm$(m^3/s)^{0,5}/m^{0,75}$]
Pelton	1 - 20 (with one jet)
Francis	20 - 140

In addition, the speed number is given by:

$$\nu=\omega\frac{(Q/\pi)^{\frac{1}{2}}}{(2gH)^{\frac{3}{4}}}=0,00633N_q \tag{6}$$

where ω is the angular speed.

The hydraulic power can be expressed as follows:

$$P_h=\rho g H Q \tag{7}$$

The output power of the turbine is given by:

$$P_s=T\omega \tag{8}$$

The turbine efficiency is formulated as follows:

$$\eta=\frac{P_s}{P_h} \tag{9}$$

4.1.1 Francis Turbine

The Francis turbine is dimensioned accounting for the reference data of the existing test bench of the Francis turbine (School of Engineering, 2022) and, inter alia, the book (Peng, 2008). The blade number of the Francis turbine runner is determined:

$$Z=250N_s^{\frac{1}{3}} \tag{10}$$

Moreover, the jet flow velocity at the outlet of the penstock can be formulated as follows:

$$v=\sqrt{2\eta_n gH} \tag{11}$$

where η_n is the velocity coefficient accounting of the losses through the penstock.

The outer diameter of the Francis turbine is determined using the method described in (Peng, 2008).

Concerning the cavitation phenomenon of the Francis turbine, it takes place at the turbine discharge, where the pressure is minimum. The Thomas cavitation factor (Peng, 2008) is used and it can be written by:

$$\sigma = 0.006 + 0.55\left(\frac{N_{sp}}{100}\right)^{1.8} \quad (12)$$

Furthermore, the critical cavitation factor for the Francis turbine is formulated as follows:

$$\sigma_c = 0.625\left(\frac{N_s}{380.78}\right)^2 \quad (13)$$

Thus, to avoid the cavitation, the Thomas cavitation factor must be more than the critical cavitation factor.

4.1.2 Cross-flow Turbine

The dimensioning of the runner of the cross-flow turbine is accomplished basing on the reference data of the existing test bench (School of Engineering, 2022) and using the developed approaches in (Birhanu et al., 2017; Desai et al., 1994; Mockmore et al., 1949). The relevant reference data for the cross-flow turbine are given in Table 3.

The dimensioning of the runner of the cross-flow turbine is accomplished basing on the reference data of the existing test bench (School of Engineering, 2022) and using the developed approaches in (Birhanu et al., 2017; Desai et al., 1994; Mockmore et al., 1949). The inner diameter of the turbine runner is selected between 55 % and 66 % of the outer diameter. In this study 66% of the outer diameter is chosen. Figure 3 illustrates the blades including the main parameters of the runner of the cross-flow turbine that can be calculated using Equations 14-20:

$$c = \sqrt{R_1^2 + R_2^2 - 2R_1R_2\cos(\beta_1 + \beta_2)} \quad (14)$$

$$\varepsilon = \arcsin\left[\frac{R_2\sin(\beta_1 + \beta_2)}{c}\right] \quad (15)$$

$$\xi = 180° - (\beta_1 + \beta_2 + \varepsilon) \quad (16)$$

$$\phi = (\beta_1 + \beta_2) - (180° - 2\xi) \quad (17)$$

$$d = \frac{R_1 \sin f}{2\sin(180° - \xi)} = 180° - 2(\beta_1 + \varepsilon) \quad (18)$$

$$r_b = \frac{d}{\cos(\beta_1 + \varepsilon)} \quad (19)$$

$$r_p = \sqrt{r_b^2 + R_1^2 - 2r_bR_1\cos\beta_1} \quad (20)$$

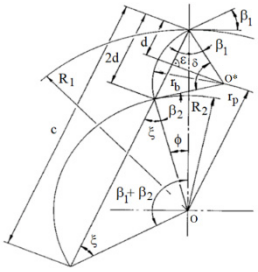

Figure 3: Runner blade (Mockmore et al., 1949).

4.1.3 Pelton Turbine

The Pelton turbine parameters are determined basing on the reference data of the existing test bench (School of Engineering, 2022) and the articles (Dandekar et al., 1979; Inversin, 1981; Jeffery, 1989; Eisenring, 1991; Santolin et al., 2009; and Zidonis, 2015). The relevant parameters of the Pelton turbine shown in Figure 4 (Eisenring, 1991) can be written as follows:

The absolute jet speed:

$$c_1 = \sqrt{2g\eta_n H} \quad (21)$$

where η_n is the velocity coefficient.

The jet diameter:

$$d = \sqrt{4Q(\pi c_1)^{-1}} \quad (22)$$

The blade width:

$$b = 2.5d \text{ à } 3.2d \quad (23)$$

The bucket height including h_1 and h_2:

$$h = 2.1d \text{ to } 2.7d$$
$$h_1 = 0.1d \text{ to } 0.35d \quad (24)$$
$$h_2 = 0.85d \text{ à } 1.5d$$

The bucket depth:

$$t \simeq 0.9d \quad (25)$$

The runner diameter:

$$D = 60u_1 i(\pi n_G)^{-1} \quad (26)$$

where i is the transmission ratio.

The rotating speed:

$$n_G = 60u_1 i(\pi D)^{-1} \quad (27)$$

The blade opening:

$$a = 1.2d \quad (28)$$

The allowance radium:

$$k \simeq (0.1 \ldots 0.17)D \quad (29)$$

The bucket number :

$$z = \pi D(2d)^{-1} \quad (30)$$

The outer diameter of turbine runner:

$$D_0 = D + 1.2h \quad (31)$$

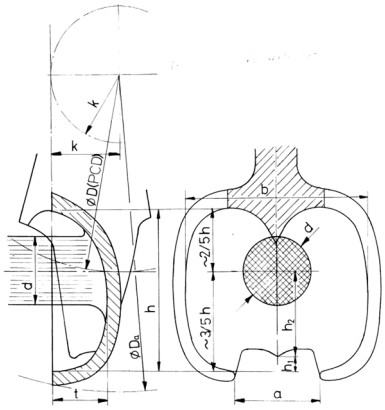

Figure 4: Bucket parameters (Eisenring, 1991).

4.2 Turbine Runner Modeling and Simulation Steps

Figure 5 shows the modeling and the simulation steps of the Francis turbine, the cross-flow turbine and the Pelton Turbine using the Inventor and the ANSYS softwares (modules: Spaceclain, CFX-Pre, CFX-Solver and CFX-Post) and accounting for the boundary conditions.

Figure 5: Turbine runner modeling and simulation steps.

5 RESULTS AND DISCUSSION

The numerical simulations are accomplished to validate the developed approach, and to analyze the effects of the draft tube length of the Francis turbine and the jet width of the cross-flow turbine on the output power and the efficiency. Tables 2-3 indicate the parameter data used for the three turbine runners after sizing.

Table 2: Parameter data for the Francis turbine.

Parameter	Value
Speed number	0.1344
Flow coefficient	0.1864
Energy coefficient	5.2095
Specific diameter	3.5
Outer diameter [m]	0.0819
Blade number	11
Height of the turbine center above the tail water level [m]	8.8
Output power [kW]	0.5884
Hydraulic power [kW]	0.6194
Liquid flow velocity in the penstock [m/s]	14.6908
Specific speed in terms of the output power	76.0666
Specific speed in terms of the flow rate	21.2279

Table 3: Parameter data of the cross-flow turbine.

Parameter	Value
Outlet blade angle [°]	50
Inner diameter [m]	0.11088
Jet thickness [m]	0.009
Runner width [m]	0.06
Blade width [m]	0.01
Blade number	14
Injector width [m]	0.04
Blade arc radius r_b [m]: Figure 3	0.027384
Radius r_p [m]: Figure 3	0.0618
Jet velocity [m/s]	14.0071
c [m] (Equation 14)	0.1154
ε [°] (Equation 15)	26.8385
ξ [°] (Equation 16)	43.1615
φ [°] (Equation 17)	16.3229
d [m] (Equation 18)	0.0173
r_b [m] (Equation 19)	0.0188
r_p [m] (Equation 20)	0.0667

Table 4: Parameter data of the Pelton turbine.

Parameter	Value
Jet flow velocity [m/s]	16.242
Nozzle coefficient	0.96 – 0.98
Jet diameter [m]	0.0229
Jet circumferential velocity [m/s]	8.1210
Circumferential velocity coefficient	0.45 - 0.49
Bucket width [m]	0.0572
Bucket height [m]	0.0492
Lower height [m]	0.0046
Upper height [m]	0.0205
Bucket number	16
Transmission ratio	0.85
Bucket depth [m]	0.0206
Tangent diameter [m]	0.2198
Bucket opening [m]	0.0274
Allowance radius [m]	0.0264
Approximate bucket number	15.0938
Runner outer diameter [m]	0.2788

5.1 Validation of the Developed Approach

The developed approach is validated using the expérimental resultats from the existing test benches for the Francis turbine, the cross-flow turbine and the Pelton turbine (Engineering School, 2022). Figures 6-11 illustrate the result comparison for the three turbines between the numerical results obtained and the experimental results for the output power and the efficiency as a function of the rotating speed. From these figures, a good agreement is found between the numerical and experimental curves.

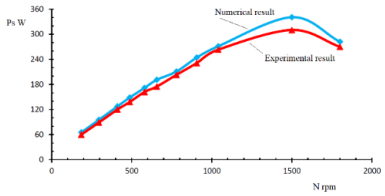

Figure 6: Output power of the Francis turbine versus rotating speed.

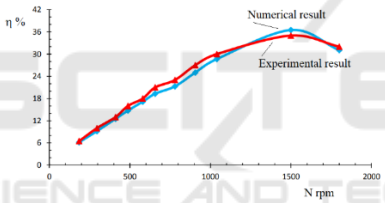

Figure 7: Efficiency of Francis turbine versus flow turbine versus rotating speed.

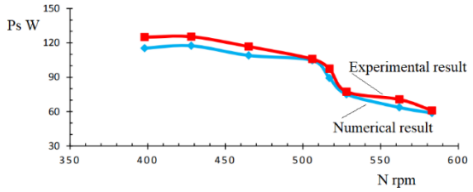

Figure 8: Output power of the cross-flow turbine versus rotating speed.

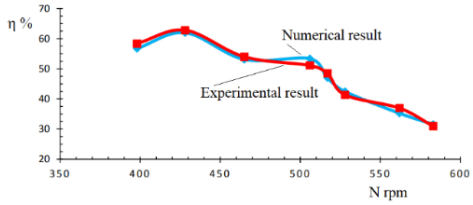

Figure 9: Efficiency of the cross-flow turbine versus rotating speed.

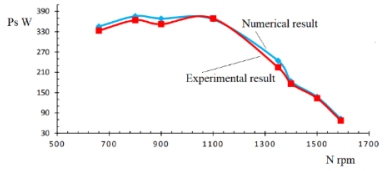

Figure 10: Output power of the Pelton turbine versus rotating speed.

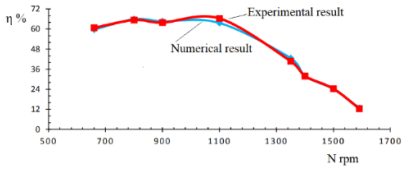

Figure 11: Efficiency of the Pelton turbine versus rotating speed.

Furthermore, the gaps achieved between both results can be explained by the fact that the numerical simulations don't take in account, inter alia, the mechanical and volumetric losses.

5.2 Effect of the Draft Tube Height of the Francis Turbine

To examine the impact of the draft tube height on the output power and the efficiency of the Francis turbine, the values of the draft tube height of 5 m, 6 m and 7 m are selected. Figures 12 and 13 show that the turbine output power and the efficiency vary little with increasing draft tube height. The increase of the height draft tube modifies the pressure difference between the inlet and the outlet of the turbine runner. This leads to rise flow velocity at the turbine runner outlet.

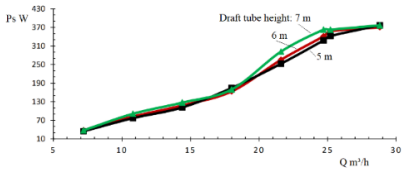

Figure 12: Output power of the Francis turbine versus flow rate.

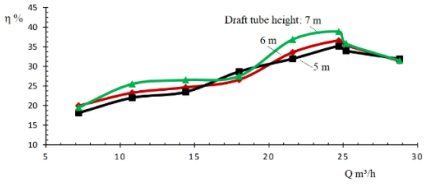

Figure 13: Efficiency of the Francis turbine versus flow rate.

5.3 Effect of the Cavitation on the Efficiency

To analyze the effect of the cavitation on the efficiency of the Francis turbine, the draft tube heights of the Francis turbine of 8.8 m without cavitation and 9.6 m with cavitation are chosen. Figure 14 illustrates the turbine efficiency curves as a function of the rotating speed. It is observed that the appearance of cavitation in the liquid flow in the turbine runner leads to the sensitive reduction of the efficiency. At the best efficiency point (B.E.P.) corresponding to 1500 rpm the relative gap is 14 % between the results with and without cavitation.

Indeed, the increase of the draft tube height causes the reduction of the static pressure due to the rise velocity of the liquid flow in the runner of the Francis turbine. This can lead to the change of the phase of the liquid water once its vapor pressure is reached. The cavitation can damage the runner of the Francis turbine in an irreversible manner. Moreover, Figure 15 depicts a high liquid flow velocity at the level of the turbine runner outlet for the case of the draft tube height of 9.6 m.

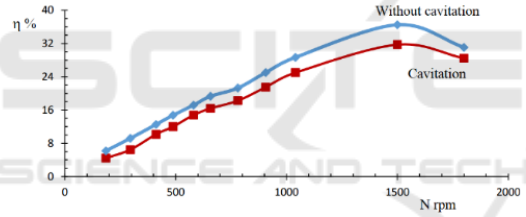

Figure 14: Efficiency of the Francis turbine versus rotating speed.

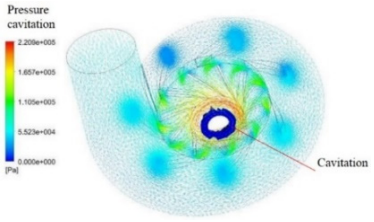

Figure 15: cavitation onset.

5.4 Effect of the Jet Width of the Cross-flow Turbine

To examine the effect of the jet width of the cross-flow turbine, the values of the jet width of 4 mm, 9 mm and 14 mm are selected. Figures 16 and 17 illustrate respectively the turbine output power and the efficiency as a function of the flow rate. From these figures, it is remarked that the output power and the efficiency with the jet width of 14 mm decrease with increasing flow rate from about 19 m³/h in comparison of the results for the jet width of 4 mm and 9 mm. The phenomenon can be explained by the fact that the water jet exerts a force on the turbine blade in rotation that is transformed in couple and in mechanical power. If the jet width varies, the flow rate changes due to the dependence of the flow rate with the section of the jet and the velocity of liquid flow. This causes the fluctuations to the level of the velocity and the jet pressure.

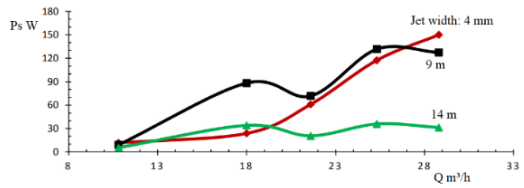

Figure 16: Output power of the cross-flow turbine versus flow rate.

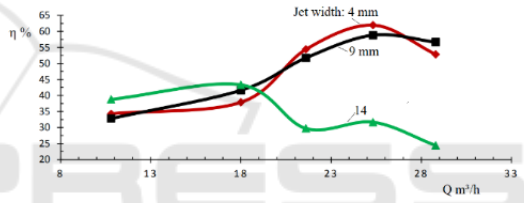

Figure 17: Efficiency of the cross-flow turbine versus flow rate.

6 CONCLUSIONS

The goal pursued in the within the framework of this research was to establish a numerical tool that would help towards the design and the modelings of the Francis turbine, cross-flow turbine and Pelton turbine for mini-hydropower stations, while based on the existing test benches for the turbine type of Francis, cross-flow and Pelton. From the reference data of the test benches in terms of the net head, the flow rate, the rotating speeds of the turbines and the equations of continuity and Navier-Stokes that govern the liquid flow in the hydraulic turbines; the numerical models of the Francis turbine, the cross-flow turbine and the Pelton turbine were designed. The numerical resolution of the equations links to the liquid flow in the turbines and the numerical simulations have been accomplished using the ANSYS-CFX code. The numerical results obtained of the output power and the efficiency were compared with those of the test benches. Thus, a good agreement was achieved between numerical

and experimental curves. In addition, the results for the effect of the draft tube height on the output power and efficiency show slight variations of the output power and efficiency. The effect of the cavitation on the efficiency of the Francis turbine was examined using the height draft tube as parameter. The highest gap of 14% was observed at the B.E.P. considering the cases with and without cavitation. Furthermore, the impact of the jet width of the cross-flow turbine on the output power and the efficiency reveals that for the higher flow rate the output power and the efficiency decrease with augmentation jet width.

ACKNOWLEDGEMENTS

The authors are grateful to the Turbomachinery Facility of the Engineering School of the University of University of Quebec in Abitibi-Témiscamingue (Rouyn-Noranda, Quebec, Canada).

REFERENCES

Alligne S., Nicolet, C., Tsujimoto, Y. et Avellan, F., 2014. Cavitation surge modelling in Francis turbine draft tube, Journal of Hydraulic Research, vol. 52, pp. 399-411.

ANSYS inc., 2022. www.ansys.com.

Bartle, A., 2002. Hydropower potential and development activities, Energy policy, vol. 30, pp. 1231-1239.

Birhanu Oliy G., Ramayya, A. V., 2017. Design and Computational Fluid Dynamic Simulation Study of High Efficiency Cross Flow Hydro-power Turbine, International Journal of Science, Technology and Society, vol. 5, pp. 120-125.

Dandekar, M., Sharma, K., 1979. Water Power Engineering: Vikas Publishing House.

Inversin, A. R., 1981. Pelton micro-hydro prototype design, ATD Research Series. vol. 1, ed: ATDI.

Desai V. R., Aziz, N. M. , 1994. An experimental investigation of cross-flow turbine efficiency," Transactions-American Society of Mechanical Engineers Journal of Fluids Engineering, vol. 116, pp. 545-545.

Eisenring M., 1991. MHPG Series, harnessing water power on small scale, Micro Pelton turbines, Volume 9. SKAT, Swiss Center for Appropriate Technology, St Gallen Switzerland and GATE, Germann Appropriate Technology Exchange, Eschborn, Germany.

Elbatran, A. H. , Yaakob, O. B., Ahmed, Y. M. et Shabara, H. M., 2015. Operation, performance and economic analysis of low head micro-hydropower turbines for rural and remote areas: A review. Renewable and Sustainable Energy Reviews, vol. 43, pp. 40-50.

Kaewnai S., and S. Wongwises, S., 2011. Improvement of the runner design of Francis turbine using Computational Fluid Dynamics, American J. of Engineering and Applied Sciences, vol. 4, pp. 540-547.

Malonda, P. Z., Dituba Ngoma, G., Ghié, W., Erchiqui, F., Kabeya, P., 2021, Characterization of a Vertical Submersible Six-Stage Pump: Accounting for the Induced Forces and Stresses. 11th International Conference on Simulation and Modeling Methodologies, Technologies and Applications (SIMULTECH).

Mockmore, C. A., Merryfield, F.,1949. The Banki Water-turbine: Engineering Experiment Station, Oregon State System of Higher Education, Oregon State College.

Jeffery N., 1989. Local Experience with Micro-Hydro Technology, ed: Alternative Technology Association.

Olgun, H., 1998. Investigation of the performance of a cross-flow turbine, International journal of energy research, vol. 22, pp. 953-964.

Olgun, H., 2000. Effect of interior guide tubes in cross-flow turbine runner on turbine performance, International Journal of Energy Research, vol. 24, pp. 953-964, 2000.

Panthee, A., Neopane, H. P., and Thapa, B., 2014 "CFD Analysis of Pelton Runner," International Journal of Scientific and Research Publications, vol. 4, pp. 1-6.

Peng, W. W., 2008. Fundamentals of turbomachinery: John Wiley & Sons.

Santolin, A., Cavazzini, G., Ardizzon G., Pavesi, G., 2009. Numerical investigation of the interaction between jet and bucket in a Pelton turbine, Proceedings of the Institution of Mechanical Engineers, Part A: Journal of Power and Energy, vol. 223, pp. 721-728.

School of Engineering, Turbomachinery laboratory (E-216), 2022. University of Quebec in Abitibi-Témiscamingue (UQAT), www.uqat.ca.

Trivedi, C., Iliev, I., Dahlhaug, O. G., Markov Z., Engstrom, F., Lysaker, H., 2020. Investigation of a Francis turbine during speed variation: Inception of cavitation. Renewable Energy 166, 147-162.

Zanette, J., Imbault D., and Tourabi, A., 2010. A design methodology for cross flow water turbines, Renewable Energy, vol. 35, pp. 997-1009.

Zhang, Z., 2016, Pelton Turbines: Springer.

Zidonis, A., 2015. Optimisation and efficiency improvement of pelton hydro turbine using computational fluid dynamics and experimental testing, Thesis, Lancaster University.

Židonis A. and Aggidis, G. A. , 2015. State of the art in numerical modelling of Pelton turbines, Renewable and Sustainable Energy Reviews, vol. 45, pp. 135-144.